Optical Engineering

OpticalEngineering.SPIEDigitalLibrary.org

Aberrated beam propagation through turbulence and comparison of Monte Carlo simulations to field test measurements

Nelofar Mosavi
Charles Nelson
Brian S. Marks
Bradley G. Boone
Curtis R. Menyuk

SPIE.

Optical Engineering 53(8), 086108 (August 2014)

Aberrated beam propagation through turbulence and comparison of Monte Carlo simulations to field test measurements

Nelofar Mosavi,[a,b,*] Charles Nelson,[c] Brian S. Marks,[a] Bradley G. Boone,[a] and Curtis R. Menyuk[b]
[a]Johns Hopkins University Applied Physics Laboratory, 11100 Johns Hopkins Road, Laurel, Maryland 20723, United States
[b]University of Maryland, Baltimore County, 1000 Hilltop Circle, Baltimore, Maryland 21250, United States
[c]United States Naval Academy, 121 Blake Road, Annapolis, Maryland 21402, United States

Abstract. Optical beam spread and beam quality factor in the presence of both an initial quartic phase aberration and atmospheric turbulence are studied. We obtain the analytical expressions for both beam radius-squared and the beam quality factor using the moment method, and we compare these expressions with the results from Monte Carlo simulations, which allow us to mutually validate the theory and the Monte Carlo simulation codes. We then analyze the first- and second-order statistical moments of the fluctuating intensity of a propagating laser beam and the probability density function versus intensity as the beam propagates through a turbulent atmosphere with constant C_n^2. At the end, we compare our analytical expression and our simulations with field test experimental results, and we find a good agreement.
[DOI: 10.1117/1.OE.53.8.086108]

Keywords: free-space optical communications; atmospheric turbulence; aberrations; Monte Carlo simulations.

Paper 140637P received Apr. 18, 2014; revised manuscript received Jul. 18, 2014; accepted for publication Jul. 21, 2014; published online Aug. 19, 2014.

1 Introduction

Free-space optical communication links support both commercial and military applications due to their high bandwidth and high directivity, which makes them hard to detect, intercept, and jam. However, a laser beam propagating in free space can undergo significant random intensity fluctuations due to turbulence along the propagation path. Also, the transverse beam quality of a laser beam is degraded by an initial quartic phase aberration. A quartic phase aberration, more commonly known as a spherical aberration, can result from aberrated optical components such as a beam-expanding telescope, focusing or collimating lenses, or other conventional optical elements.[1] In general, an initial quartic aberration of the beam and atmospheric turbulence lead to far-field beam spread, degrade the laser beam focusability, and increase values of the beam quality factor. The beam spread and beam quality factor for a fully coherent beam[2,3] and a partially coherent beam[4,5] in the presence of atmospheric turbulence have been previously studied. Also, the beam quality factor in the presence of aberrations has been described by Siegman[1] and Siegman and Ruff.[6] In this paper, we study the spread and beam quality factor in the presence of both atmospheric turbulence and an initial quartic aberration. We obtain the analytical expressions for both the mean-square beam radius and the beam quality factor using the moment method, and we compare these expressions with the results from Monte Carlo simulations. This comparison allows us to mutually validate the theory and the Monte Carlo simulation codes. We then analyze the first- and second-order statistical moments of the fluctuating intensity of a propagating laser beam and the probability density function (PDF) versus the intensity at the detector point. We show that in the presence of moderate to strong turbulence fluctuations, the simulation data fit well to a gamma-gamma PDF. At the end, we compare our analytical expression and our simulations with the field test experimental results, and we find a good agreement.

This paper is organized as follows: In Sec. 2, we review the theory of beam spreading in the presence of both quartic beam aberrations and atmospheric turbulence.[7] We use the moments method to evaluate the mutual coherence function, and we obtain an exact analytical expression for the ensemble-averaged mean-square beam radius, $\langle\overline{r^2}\rangle$. We also calculate the beam quality factor, and we show that it has the form $M^4_{\text{total}} = 1 + M^4_{\text{ab}} + M^4_{\text{turb}}$, where M^4_{ab} and M^4_{turb} are due to initial aberrations and turbulence, respectively, indicating that the contribution of the turbulence, M^4_{turb}, to the beam quality is strictly additive. We describe the Monte Carlo simulations, and we look at the beam radius versus propagation distance in order to compare the analytical results with the Monte Carlo simulations.

Experimental field tests were conducted near Wallops Island, Virginia, and are described in Sec. 3. We look at the intensity fluctuations due to the optical turbulence along the propagation path, the PDF, and the scintillation index of the field test data and compare these results with our Monte Carlo simulations of Gaussian beam propagation through a turbulent atmosphere, and we find a good agreement.

*Address all correspondence to: Nelofar Mosavi, E-mail: nelofar.mosavi@jhuapl.edu

0091-3286/2014/$25.00 © 2014 SPIE

2 Beam Spreading in Presence of Both Quartic Beam Aberrations and Atmospheric Turbulence and Monte Carlo Simulations

2.1 *Analytical Expressions*

The classical approach for calculating the ensemble-averaged mean-square beam radius in a turbulent atmosphere described in Andrews and Phillips[8] and Fante,[9] is to find a good analytical approximation for the mutual coherence function and then to carry out an integration over the transverse beam profile. This approach works well with Gaussian beams, but is not useful for aberrated beams where good analytical approximations for the mutual coherence function are difficult to obtain. Therefore, it is advantageous to use other approaches such as the moment method that is described by Feizulin and Kravtsov[2] and by Gbur and Wolf.[4] We previously presented an application of this approach to calculate the mean-square beam radius for a beam with an initial quartic phase aberration as it propagates through the atmosphere.[7] We review the principal elements of this theory that will be needed in the remainder of the paper. We note that the moment method allows us to directly obtain an exact analytical expression for the ensemble-averaged mean-square beam radius, $\langle\overline{r^2}\rangle$, without requiring us to obtain an expression for the mutual coherence function.

We first write the paraxial wave equation[8]

$$2ik\frac{\partial V(\mathbf{R})}{\partial z}+\nabla_T^2 V(\mathbf{R})+2\,k^2 n_1(\mathbf{R})V(\mathbf{R})=0, \tag{1}$$

where $\mathbf{R}=(\mathbf{r},z)$ is the position vector, $\mathbf{r}=(x,y)$ is the transverse vector, z is the propagation distance, k is the wavenumber of the light, $V(\mathbf{R})$ is the envelope of the electric field, ∇_T^2 is the transverse Laplacian operator, and $n_1(\mathbf{R})$ is the randomly fluctuating portion of the atmosphere's refractive index. We discuss the solution to the paraxial wave equation in the next section.

We will consider here an aberrated Gaussian beam with a quartic phase aberration that has been described by Siegman[1] and Siegman and Ruff.[6] We may write the initial beam profile as

$$V_0(\mathbf{r})\equiv V(\mathbf{r},z=0)=A\,\exp\left(-\frac{r^2}{W_0^2}\right)\exp\left[ik\left(\frac{r^2}{2F}-C_4r^4\right)\right], \tag{2}$$

where $r=|\mathbf{r}|$ is the magnitude of the transverse vector, W_0 is the initial beam radius, C_4 is the aberration strength of the nonideal optical element, and F is the beam focal length. The quantity A is the amplitude, and we may set $A=1$ for simplicity, since our system is linear. The case in which the beam radius is a minimum at $z=0$ will be presented here. In that case, we find

$$\frac{1}{2F}=\frac{2\overline{r^4}}{\overline{r^2}}C_4=2C_4W_0^2, \tag{3}$$

where the overbar indicates an average over the beam intensity, so that

$$\overline{r^n}(z)=\frac{\iint_{-\infty}^{\infty}\mathrm{d}^2r\,r^nI(\mathbf{r},z)}{\iint_{-\infty}^{\infty}\mathrm{d}^2r\,I(\mathbf{r},z)}, \tag{4}$$

where we let $I(\mathbf{r},z)=|V(\mathbf{r},z)|^2$. Writing $\mathbf{r}=(r,\theta)$ in cylindrical coordinates, we note that $I(\mathbf{r},z)$ is not independent of θ for particular realizations. In contrast, we will denote the ensemble average over all turbulence realizations using the brackets $\langle\cdot\rangle$, and $\langle I(\mathbf{r},z)\rangle$ is independent of θ, since the initial profile that we considered is θ-independent.

Using Eqs. (2) and (3), we find that the initial wave function of a Gaussian-distributed beam with quartic phase aberration becomes

$$V_0(\mathbf{r})=\exp\left[-\frac{r^2}{W_0^2}+ikC_4(2r^2W_0^2-r^4)\right]. \tag{5}$$

The beam radius squared $W^2(z)$ is traditionally defined as twice the mean-square radius, and it can be written as

$$\begin{aligned}\langle W^2(z)\rangle=2\langle\overline{r^2}\rangle&=2\frac{\iint_{-\infty}^{\infty}\mathrm{d}^2r\,r^2\Gamma_2(\mathbf{r},\mathbf{r},z)}{\iint_{-\infty}^{\infty}\mathrm{d}^2r\,\Gamma_2(\mathbf{r},\mathbf{r},z)}\\&=2\frac{\iint_{-\infty}^{\infty}\mathrm{d}^2r\,r^2\langle I(\mathbf{r},z)\rangle}{\iint_{-\infty}^{\infty}\mathrm{d}^2r\langle I(\mathbf{r},z)\rangle},\end{aligned} \tag{6}$$

where $\Gamma_2(\mathbf{r},\mathbf{r},z)$ is the mutual coherence function. In writing $\Gamma_2(\mathbf{r},\mathbf{r},z)$, we follow Andrews and Phillips and use the scalar field $U(\mathbf{r},z)=V(\mathbf{r},z)\exp(ikz)$, rather than the envelope $V(\mathbf{r},z)$. Defining $U_0(\mathbf{r})\equiv U(\mathbf{r},z=0)$, we also have $U_0(\mathbf{r})=V_0(\mathbf{r})$. We now find that the mutual coherence function can be written as[8]

$$\begin{aligned}\Gamma_2(\mathbf{r},\mathbf{r},z)=\left(\frac{k}{2\pi z}\right)^2\iint_{-\infty}^{\infty}\mathrm{d}^2Q\iint_{-\infty}^{\infty}\mathrm{d}^2S\,U_0\left(S+\frac{Q}{2}\right)\\U_0^*\left(S-\frac{Q}{2}\right)\exp\left[\frac{ik}{z}(\mathbf{S}-\mathbf{r})\cdot\mathbf{Q}\right]\quad\times\exp\left[-\frac{1}{2}D_{\mathrm{sp}}(Q)\right],\end{aligned} \tag{7}$$

where $D_{\mathrm{sp}}(Q)$ is the turbulence structure function, $Q=|\mathbf{Q}|$, $S=|\mathbf{S}|$, and $\mathbf{S}$ and $\mathbf{Q}$ are two-dimensional dummy variables. In our computational work, we will use the von Karman–Tatarskii model[10] of turbulence. In this case, we find that when $Q\to 0$, then $D_{\mathrm{sp}}(Q)$ is well approximated by[8]

$$\begin{aligned}D_{\mathrm{sp}}(Q)=1.09C_n^2k^2zl_0^{-1/3}Q^2[(1+Q^2/l_0^2)^{-1/6}\\-0.72(k_0l_0)^{1/3}],\end{aligned} \tag{8}$$

where C_n is the refractive-index structure parameter, l_0 is the inner scale of the turbulence, and $k_0=2\pi/L_0$. where L_0 is outer scale of turbulence. We see that when $Q\to 0$, then $D_{\mathrm{sp}}(Q)\propto Q^2$. That is the case for any physically reasonable turbulence model, not just the von Karman–Tatarskii model, as we have previously shown.[7]

Substituting Eq. (5) into Eq. (7) results in

$$\begin{aligned}\Gamma_2(\mathbf{r},\mathbf{r},z)=\left(\frac{k}{2\pi z}\right)^2\int\!\!\int_{-\infty}^{\infty}\mathrm{d}^2Q\int\!\!\int_{-\infty}^{\infty}\mathrm{d}^2S\exp\left(\frac{2S^2}{W_0^2}-\frac{Q^2}{2W_0^2}\right)\\\times\exp\left\{\frac{ik}{z}[1+C_4z(4W_0^4-4S^2-Q^2)]\mathbf{S}\cdot\mathbf{Q}-\frac{ik}{z}\mathbf{r}\cdot\mathbf{Q}\right\}\\\times\exp\left[-\frac{1}{2}D_{\mathrm{sp}}(Q)\right].\end{aligned} \tag{9}$$

Even when turbulence is absent so that $D_{sp}(Q) = 0$, Eq. (9) cannot be analytically evaluated. However, the beam radius squared may be found using the moments method starting from Eq. (6). To do so, we first calculate G_0

$$G_0 \equiv \iint_{-\infty}^{\infty} \mathrm{d}^2 r \Gamma_2(\mathbf{r}, \mathbf{r}, z) = \left(\frac{k}{2\pi z}\right)^2 \frac{\pi}{2} W_0^2. \tag{10}$$

Next, we calculate G_2 when there is no turbulence, so that

$$G_2 \equiv \iint_{-\infty}^{\infty} \mathrm{d}^2 r r^2 \Gamma_2(\mathbf{r}, \mathbf{r}, z) = \left(\frac{k}{2\pi z}\right)^2 \left[\frac{\pi}{4} W_0^4 + \frac{\pi z^2}{k^2}(1 + 2\ k^2 C_4^2 W_0^8)\right]. \tag{11}$$

Therefore, the beam radius squared in the absence of turbulence becomes

$$W^2(z) = 2\overline{r^2} = 2\frac{G_2}{G_0} = W_0^2 + \frac{4z^2}{k^2 W_0^2}(1 + 2\ k^2 C_4^2 W_0^8), \tag{12}$$

so that the beam quality factor due to quartic aberrations is given by $M_{ab}^2 = 2\ k^2 C_4^2 W_0^8$. This result is consistent with the earlier calculations of Siegman[1] and of Siegman and Ruff.[6]

Adding the turbulence contribution to the total beam radius squared, we obtain

$$\langle W^2(z)\rangle = 2\langle\overline{r^2}\rangle = 2\frac{G_2}{G_0} = W_0^2 + W_{diff}^2 + \langle W_{turb}^2\rangle + W_{ab}^2, \tag{13}$$

where $W_{diff}^2 = 4z^2/k^2 W_0^2$, $\langle W_{turb}^2\rangle = 2.18 C_n^2 l_0^{-1/3} z^3$, and $W_{ab}^2 = 8z^2 C_4^2 W_0^6$. In the absence of aberrations, this equation is consistent with that in Ref. 2.

The turbulent contribution to M_{total}^4 for all distances is given by

$$M_{turb}^2 = \frac{k^2 W_0^2}{4z^2}(2.18 C_n^2 l_0^{-1/3} z^3) = 0.505 C_n^2 l_0^{-1/3} k^2 W_0^2 z, \tag{14}$$

so that in total

$$M_{total}^4 = 1 + M_{ab}^4 + M_{turb}^4. \tag{15}$$

2.2 *Monte Carlo Simulations*

We also calculated the beam-radius-squared, $\langle W^2\rangle_{MC} = 2\langle\overline{r^2}\rangle_{MC}$, using the Monte Carlo technique, where $\langle\cdot\rangle_{MC}$ denotes the ensemble average of the Monte Carlo realizations. The solution of the wave equation, Eq. (1), over a small Δz can be written as

$$U(\mathbf{r}, z + \Delta z) = U(\mathbf{r}, z) \exp\left[ik \int_0^{\Delta z} \mathrm{d}z' n_1(\mathbf{r}, z')\right], \tag{16}$$

where we recall $U(\mathbf{r}, z) = V(\mathbf{r}, z)\exp(ikz)$. We then write the first two statistical moments of the phase screens $\theta \equiv k\int_0^{\Delta z} \mathrm{d}z' n_1(\mathbf{r}, z')$ as

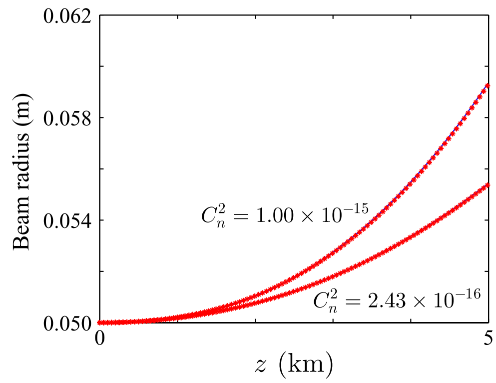

Fig. 1 The solid lines (–) indicate the exact result Eq. (12), and stars (*) indicate the Monte Carlo simulations.

$$\langle\theta\rangle = k \int_0^{\Delta z} \mathrm{d}z' \langle n_1(\mathbf{r}, z')\rangle = 0 \tag{17}$$

and

$$\langle\theta^2\rangle = k^2 \int_0^{\Delta z} \mathrm{d}z' \int_0^{\Delta z} \mathrm{d}z'' \langle n_1(\mathbf{r}, z') n_1(\mathbf{r}, z'')\rangle. \tag{18}$$

We use the method of randomly varying phase screens,[11] combined with the split-step method,[11] to calculate $U(\mathbf{r}, z)$ for a particular realization and from that we calculate $\overline{r^2} = \iint_{-\infty}^{\infty} \mathrm{d}^2\mathbf{r} r^2 |U(\mathbf{r}, z)|^2 / \iint_{-\infty}^{\infty} \mathrm{d}^2\mathbf{r} |U(\mathbf{r}, z)|^2$. We use the von Karman–Tatarskii spectrum[10] to obtain the spectrum of the phase screens. Averaging over 10^4 realizations, we obtain an estimate $\langle W^2(z)\rangle_{MC} = 2\langle r^2(z)\rangle_{MC}$. Figure 1 compares Eq. (13) with the Monte Carlo simulations, setting $W_0 = 5$ cm, $l_0 = 30$ mm, $C_4 = 0.08\ \mathrm{m}^{-3}$, and $\lambda = 1550$ nm. The agreement between the simulation and the analytical expression is excellent, mutually validating our simulations and our analytical expressions.

3 Experimental Results Compared with Monte Carlo Simulations

Figure 2 presents the spatial profiles at three different propagation distances of an infrared laser beam at 1550 nm on a 120 cm by 120 cm screen in the maritime environment captured off the Atlantic coast near Wallops Island, Virginia.[12] The beam is collimated and the receiver and transmitter are both on-axis. These results can be compared with Fig. 3, which shows the infrared (IR) spatial profiles of a Gaussian beam on a 80 cm by 80 cm screen with over 10^4 iterations using Monte Carlo simulations at three different propagation distances of 5.1, 10.7, and 17.8 km. Since we show the single realizations of the experimental beams, the simulations do not exactly reproduce the experimental results. We see, however, that the spread of the beam in both the experiments and the simulations is occurring on the same length scale.

For the field experiment, a bidirectional infrared optical link was established between a lookout tower and a research vessel that is located in a range between about 5 km away from the lockout tower and almost the optical horizon distance of 17.8 km. The link was locked, and pointing and tracking were maintained using commercially available adaptive optics terminals. The data that are presented here were collected from the 2.54 cm diameter power-in-fiber

Fig. 2 Infrared spatial profiles of the propagating beam from data collected near Wallops Island, Virginia.[10] (a) 5.1 km. (b) 10.7 km. (c) 17.8 km.

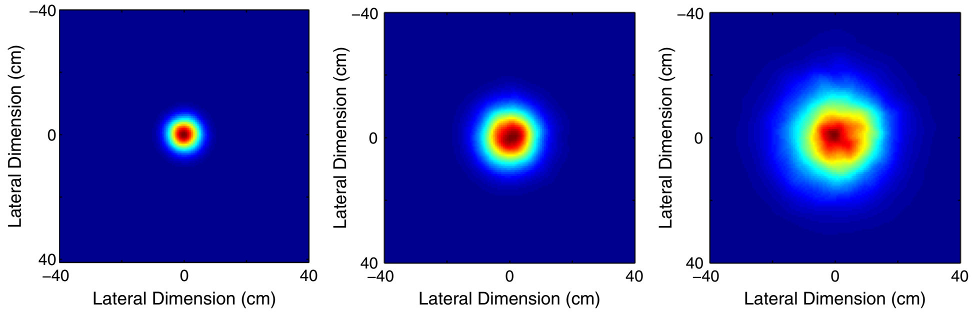

Fig. 3 IR spatial profiles of a Gaussian beam using Monte Carlo simulations averaged over 10^4 realizations at three different propagation distances: (a) 5.1 km, (b) 10.7 km, and (c) 17.8 km.

adaptive optics detector on the research vessel, and the beam from the tower was transmitted from a 10-cm adaptive optics aperture. Observed realizations are each 1-min long, samples of the data were collected at 10^4 samples/second or 6×10^5 data points for the 1-min observation time, and then normalized to the mean of the data. The experiments that we report here used adaptive optics; however, we have experimentally compared the statistics using 0.64-cm power-in-bucket located just off of the centerline,[13] and the adaptive optics do not appear to have significant impact on the beam quality statistics that we report here. We carried out the simulations setting $F = 0$. We found that we had to use $C_n^2 = 1.2 \times 10^{-15}$ m$^{-2/3}$ at a propagation distances of 5.1 and 17.8 km and $C_n^2 = 4.0 \times 10^{-16}$ m$^{-2/3}$ at a propagation distance of 10.7 km to obtain a good agreement between our simulations and experiments. These values differ somewhat from the path average value of 2.4×10^{-15} m$^{-2/3}$ that was estimated at the time of the experiments, but are within the error range of this estimate. This estimate was rough, and, in fact, comparison to Monte Carlo simulations like ours is an effective means of deducing the actual value. We note that it is possible that C_n^2 fluctuates during the data runs and may be partially affected by the diurnal cycle. However, it has been previously shown that we may assume that the value is constant across the link.[12] Additional details of the experimental setup as well as the overall environmental characterizations can be found in Refs. 14 and 15.

Additionally, in Fig. 4, we show a comparison of the Monte Carlo simulations with the field test data at a propagation distance of 17.8 km with both the lognormal and gamma-gamma PDF distributions.[12] With moderate to strong turbulence fluctuations, the gamma-gamma PDF should agree well with both our simulations and experiments. The fluctuation regime is characterized by the Rytov variance[8]

$$\sigma_R^2 = 1.23 C_n^2 k^{7/6} z^{11/6}. \tag{19}$$

The weak fluctuation regime corresponds to $\sigma_R^2 < 1$, whereas the moderate-to-strong fluctuation regime corresponds to $\sigma_R^2 > 1$. For our simulations, the Rytov variance is 4.7, and, for the experiments it is 10.5 at 17.8 km; so, we are in the moderate to strong fluctuation regime. Our results are consistent with those in Ref. 13.

Table 1 shows a comparison of the scintillation index that we obtain from our Monte Carlo simulations and from our experiments. The scintillation index is the irradiance variance scaled by the square of the mean irradiance[8]

$$\sigma_I^2(\mathbf{r}, z) = \frac{\langle I^2(\mathbf{r}, z)\rangle}{\langle I(\mathbf{r}, z)\rangle^2} - 1, \tag{20}$$

where the irradiance is equal to mutual coherence function, $\langle I(\mathbf{r}, z)\rangle = \Gamma_2(\mathbf{r}, \mathbf{r}, z)$, and the second moment of the irradiance is the fourth-order coherence function, $\langle I^2(\mathbf{r}, z)\rangle = \Gamma_4(\mathbf{r}, \mathbf{r}, \mathbf{r}, \mathbf{r}, z)$. In order to calculate the scintillation index of the simulation, we computed the irradiance from the peak intensity over 10^4 realizations. In the experiments, the scintillation index is computed directly from the data run. As can be seen in Table 1, the scintillation increases as distance increases. The agreement between the simulations and experimental results is good for all distances. As was mentioned previously, we found that we had to use $C_n^2 = 1.2 \times 10^{-15}$ m$^{-2/3}$ at a propagation distances of 5.1 and 17.8 km and $C_n^2 = 7.0 \times 10^{-16}$ m$^{-2/3}$ at a propagation distance of 10.7 km to obtain a good agreement between our simulations and experiments. The results indicate the utility of using Monte Carlo simulations to obtain good estimates of the turbulence parameters.

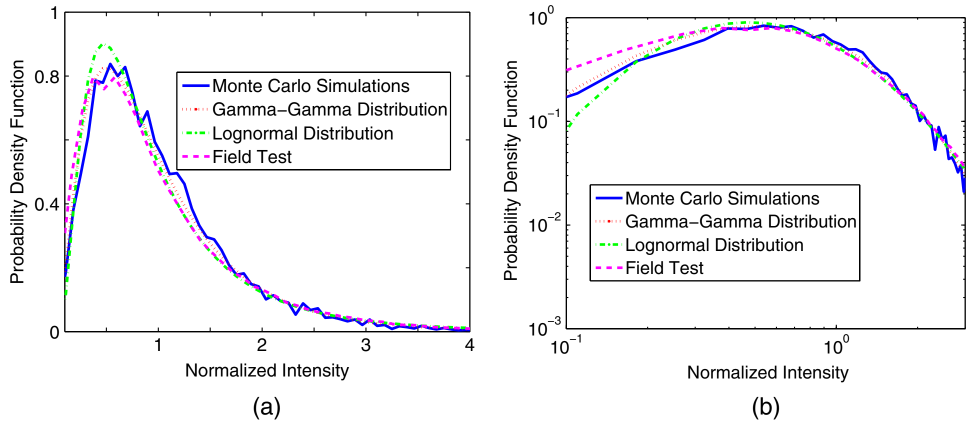

Fig. 4 Comparison of the Monte Carlo simulations and the field test at a propagation distance of 17 km with the lognormal and gamma-gamma PDF models. (a) Probability of intensity versus normalized intensity. (b) Log probability of intensity versus log normalized intensity.

Table 1 Simulation versus field test.

	Scintillation index	
Distance (km)	Simulations	Experiment
5.1	0.066	0.066
10.7	0.127	0.123
17.8	0662	0.635

4 Conclusion

In conclusion, we reviewed analytical expressions for both the mean-square beam radius and the beam quality factor using the moment method that was first developed by Feizulin and Kravtsov. These analytical expressions help us to understand how the laser beam spreads and degrades in passing through atmospheric turbulence when there is an initial quartic aberration. We compared these expressions with the results from Monte Carlo simulations, which allowed us to mutually validate the theory and our Monte Carlo codes. Monte Carlo simulations have been used far less in the studies of free-space communication systems than in optical-fiber communication systems, but they are likely to become an indispensable tool in the future as systems grow more complex. We have shown that the probability distribution of the simulation predicts a gamma-gamma distribution in agreement with experiments. Additionally, we compared the simulation results with field test data. The agreement was excellent. In particular, we obtained good agreement between the scintillation index that is found experimentally and the scintillation index that is calculated in our simulations. Our results also indicate the usefulness of the Monte Carlo simulations as a way to both understand the experimental behavior and estimate the turbulence parameters.

Acknowledgments

This work was supported by the Johns Hopkins University Applied Physics Laboratory through an IRAD grant. The authors would like to acknowledge useful discussions with F. Davidson, R. Sova, and W. Torruellas.

References

1. A. E. Siegman, "Analysis of laser beam quality degradation caused by quartic phase aberrations," *Appl. Opt.* **32**(30), 5893–5901 (1993).
2. Z. I. Feizulin and Y. A. Kravtsov, "Broadening of laser beam in a turbulent medium," *Radiophys. Quantum Electron.* **10**(1), 33–35 (1967).
3. M. H. Mahdieh, "Numerical approach to laser beam propagation through turbulent atmosphere and evaluation of beam quality factor," *J. Opt. Commun.* **281**(13), 3395–3402 (2008).
4. G. Gbur and E. Wolf, "Spreading of partially coherent beams in random media," *J. Opt. Soc. Am.* **19**, 1592–1598 (2002).
5. Y. Dan and B. Zhang, "Beam propagation factor of partially coherent flat-topped beams in a turbulent atmosphere," *J. Opt. Soc. Am.* **16**(20), 15563–15575 (2008).
6. A. E. Siegman and J. Ruff, "Effect of spherical aberration on laser beam quality," *Proc. SPIE* **1834**, 130–139 (1992).
7. N. Mosavi et al., "Optical beam spreading in the presence of both atmospheric turbulence and quartic aberration," *Proc. SPIE* **8971**, 897103 (2014).
8. L. C. Andrews and R. L. Phillips, *Laser Beam Propagation Through Random Media*, SPIE Press, Bellingham, Washington (2005).
9. R. L. Fante, "Electromanetic beam propagation in turbulent media," *Proc. IEEE* **63**(12), 1669–1692 (1975).
10. V. I. Tatarskii, "The effects of the turbulent atmosphere on wave propagation," Israel Program for Scientific Translations, Jerusalem; Reproduced by National Technical Information Service, U.S. Dept. of Commerce (1971).
11. T. Poon and T. Kim, *Engineering Optics With Matlab*, World Scientific Publishing Co., Singapore (2006).
12. C. Nelson et al., "Measurements and comparison of the probability density and covariance functions of laser beam intensity fluctuations in a hot-air turbulence emulator with the maritime atmospheric environment," *Proc. SPIE* **8517**(31), 851707 (2012).
13. C. Nelson et al., "Probability density functions of power-in-bucket and power-in-fiber for an infrared laser beam propagating in the maritime environment," *Appl. Opt.* **52**, 7449–7461 (2013).
14. J. C. Juarez et al., "Free-space optical channel characterization in the maritime environment," *Proc. SPIE* **7685**, 76850H (2010).
15. C. Nelson et al., "Probability density function computations for power-in-bucket and power-in-fiber measurements of an infrared laser beam propagating in the maritime environment," *Proc. SPIE* **8038**, 80380G (2011).

Nelofar Mosavi is currently an EMC and RF engineer at Johns Hopkins University Applied Physics Laboratory, Space Department. She received her BS degree in electrical engineering from Oakland University in 2004, and an MS degree in electrical engineering from Johns Hopkins University in 2010. She is currently working toward her PhD degree at the University of Maryland Baltimore County. She previously worked for SENTEL Corporation, General Motors, DENSO International, and Molex Automotive.

Charles Nelson received his Bachelors degree in physics from the United States Naval Academy in 1996, qualified as nuclear engineer from the Navy's Nuclear Power Program in 2001, received a master's of engineering management from Old Dominion University in 2003, and a PhD degree in electrical and computer engineering from Johns Hopkins University in 2013. He is currently an assistant professor in the Electrical and Computer Engineering Department at the United States Naval Academy.

Brian S. Marks received his BS degree in mathematics and physics from North Carolina State University in 1995, and his PhD degree in applied mathematics from Northwestern University in 2000. He worked at University of Maryland Baltimore County as a research scientist for 7 years and at Indiana University Bloomington as a lecturer for 6 years. He is currently a member of the professional staff at Johns Hopkins University Applied Physics Laboratory.

Bradley G. Boone has been involved with electro-optical and infrared systems development at JHU/APL for over 36 years. Recently, he led several initiatives in optical communications for deep and near-terrestrial space applications, as well as RF and optical sensors for proximity space operations and small-body (e.g., asteroid) landing. He has done R&D work in pattern recognition, superconducting electronics, and optical signal processing, and was involved in advanced missile guidance for over two decades.

Curtis R. Menyuk received his BS and MS degrees from MIT, in 1976 and the PhD degree from UCLA, in 1981. He has been a professor in the computer science and electrical engineering at the University of Maryland Baltimore County (UMBC) since 1986. His primary research area is the theoretical and computational study of fiber optic systems. He is a member of SIAM and SPIE and a fellow of APS, the OSA, and the IEEE.